Synthesis of spinel-type lithium antimony manganese oxides and their Li$^+$ extraction/ion insertion reactions

Ramesh Chitrakar, Hirofumi Kanoh,* Yoji Makita, Yoshitaka Miyai and Kenta Ooi

Shikoku National Industrial Research Institute, 2217-14 Hayashi-cho, Takamatsu, Japan 761-0395. E-mail: chitrak@sniri.go.jp; E-mail: kano@sniri.go.jp; E-mail: ooi@sniri.go.jp

Spinel-type lithium antimony manganese oxide was first synthesized by aging the precipitates that were obtained by reaction of a mixed aqueous solution of manganese(II) and antimony(V) chlorides (Sb/Mn = 0.25) with (LiOH + H$_2$O$_2$) solution, followed by hydrothermal treatment at 120 °C. A well crystallized spinel-type solid with a chemical composition of Li$_{1.16}$Sb(V)$_{0.29}$Mn(III)$_{0.77}$Mn(IV)$_{0.77}$O$_4$ was obtained; it had the characteristic of including mixed valence manganese. The spinel structure was preserved during heating up to 600 °C. Most of the lithium ions in the prepared material could be extracted by treating with an acid; the extraction progressed topotactically, preserving the spinel structure, accompanied by a decrease in the lattice constant from 8.31 ± 0.01 Å to 8.13 ± 0.01 Å. The mean oxidation of manganese increased from 3.50 to 3.98 after acid treatment, due to the disproportionation of trivalent manganese. The DTA-TG analysis and IR spectra showed the formation of lattice protons exchangeable with lithium ions. The pH titration study showed that the acid treated sample had a remarkable lithium ion-sieve property over the entire pH range studied. The affinity order was K < Na ≪ Li and the exchange capacity reached 5.6 mmol g^{-1} for Li$^+$. It showed a selective uptake of 14 mg g^{-1} of Li$^+$ from LiCl enriched seawater.

Introduction

Hydrous oxides of tetravalent and pentavalent metals are known to possess interesting ion exchange properties.[1–4] Recently, ion-sieve type inorganic ion exchangers have attracted attention because of their remarkably high selectivity for certain ions.[4–6] Usually they can be prepared by the templating reaction, using metal ions as templates.[6] When lithium ions are used as templates, the inorganic exchangers obtained show remarkably high selectivity for the adsorption of lithium ions in the aqueous phase. Many kinds of lithium ion-sieve materials such as spinel-type manganese oxide,[7–10] titanic acid derived from Li$_2$TiO$_3$,[11] and monoclinic antimonic acid derived from LiSbO$_3$,[12] have been developed to date.

Spinel-type manganese oxide can be obtained by heat treatment of Li$^+$ doped manganese oxide followed by the removal of Li$^+$ with acid. The Li$^+$ extraction/insertion reactions of spinel-type manganese oxides have been studied extensively from a fundamental standpoint[13–21] or standpoints applicable to the development of electrode materials for lithium batteries[22–24] or lithium selective adsorbents from seawater.[10,25–27] The structure and extraction/insertion reactions vary widely depending on the preparation method and conditions. The extraction/insertion reaction of spinel-type manganese oxide can be classified into two types, redox and ion exchange types. The redox reaction is typically observed in the (LiMn$_2$O$_4$–λ-MnO$_2$) system and the ion exchange reaction in the (Li$_{1.33}$Mn$_{1.67}$O$_4$–MnO$_2$·0.31H$_2$O) system. Sample MnO$_2$·0.31H$_2$O is effective for the recovery of lithium from seawater,[28] since it has adsorption sites more acidic than λ-MnO$_2$ and has a higher chemical stability against Li$^+$ insertion/extraction in aqueous media.

Introduction of another element to the host matrix is an effective method for improving the adsorptive properties of inorganic ion exchangers. Feng *et al.*[29,30] have studied the Li$^+$ extraction and metal-ion insertion reactions with LiMg$_{0.5}$Mn$_{1.5}$O$_4$ and LiZn$_{0.5}$Mn$_{1.5}$O$_4$ spinels in the aqueous phase. The introduction of divalent metals resulted in an increase in the chemical stability of manganese oxide, since the divalent metals promote the formation of tetravalent manga-

nese in the oxide. Liu *et al.*[31] have studied the host–guest reactions with LiAlMnO$_4$ and LiFeMnO$_4$ spinels. However, there have been no reports on the preparation of spinel-type manganese oxides containing pentavalent metals and their metal ion extraction/insertion reactions. This is because the pentavalent metals tend to form stable lithium compounds like LiSbO$_3$, LiNbO$_3$, *etc.* individually instead of spinel-type lithium metal(V) manganese oxide.

In the present paper, we report the preparation of spinel-type lithium antimony manganese oxide (Sb/Mn = 0.20) by hydro-thermal reaction. We found that it has an interesting composition with mixed valence manganese. The preparation conditions of this material and its structural characteristics were investigated. In addition, the lithium extraction and metal ion insertion reactions with this material were studied by chemical analysis, measurement of the distribution coefficient and pH titration.

Experimental

Materials

A 1 M aqueous solution of manganese(II) chloride (1 M = mol dm^{-3}) was mixed with 0.5 M aqueous solution of antimony(V) chloride (Sb/Mn = 0.25). The mixed solution was concentrated by evaporation and poured into a 0.3 M lithium hydroxide solution containing 10% hydrogen peroxide in the Li/(Mn + Sb) mole ratio of 4. The precipitate was aged overnight, filtered, washed with deionized water and dried at 60 °C. The dried material (1.0 g) was mixed with 40 cm^3 of 0.1 M lithium hydroxide solution in a Teflon lined stainless steel vessel (50 cm^3) and autoclaved at 120 °C for 6 days. The product was filtered, washed with deionized water and dried at 60 °C. The heat-treated sample was obtained by heating the dried sample at 400 °C or 600 °C for 4 h in air. The products were designated as LiSbMnO-RT, LiSbMnO-400, and LiSbMnO-600 for samples dried at 60 °C, heated at 400 °C, and 600 °C, respectively.

Lithium extraction from lithium antimony manganese oxide was carried out batchwise using a 0.5 M HCl solution. A

Table 1 Composition of lithium antimony manganese oxides and their delithiated materials

Sample	Li/Mn	Sb/Mn	H_2O/Mn	Z_{Mn}	Formula	$m+x+y+z$
LiSbMnO-RT	0.75	0.19		3.50	$Li_{1.16}Sb(v)_{0.29}Mn(III)_{0.77}Mn(IV)_{0.77}O_4$	2.99
LiSbMnO-400	0.75	0.19		3.54	$Li_{1.14}Sb(v)_{0.29}Mn(III)_{0.70}Mn(IV)_{0.83}O_4$	2.96
LiSbMnO-600	0.75	0.19		3.56	$Li_{1.14}Sb(v)_{0.29}Mn(III)_{0.67}Mn(IV)_{0.85}O_4$	2.95
HSbMnO-RT	0.003	0.21	1.29	3.98	$MnO_2 \cdot 0.10Sb_2O_5 \cdot 1.3H_2O$	
HSbMnO-400	0.005	0.21	2.21	3.98	$MnO_2 \cdot 0.10Sb_2O_5 \cdot 2.2H_2O$	
HSbMnO-600	0.005	0.19	1.34	4.00	$MnO_2 \cdot 0.10Sb_2O_5 \cdot 1.3H_2O$	

product sample in powder form (2 g) was added to the HCl solution (2 dm^3) and stirred for 1 day. The precipitates were filtered and washed with deionized water and dried at 60 °C. The delithiated materials were designated as HSbMnO-RT, HSbMnO-400 and HSbMnO-600, respectively.

Chemical analysis

The powder (50 mg) was dissolved in a small amount of hydrochloric acid solution containing H_2O_2 and the lithium, manganese and antimony contents were determined by atomic absorption spectrophotometry. The mean oxidation state of manganese was evaluated after determining the available oxygen by the standard oxalic acid method.[32]

Physical analysis

X-Ray diffraction analysis was carried out using a Rigaku type RINT 1200 X-ray diffractometer with a graphite monochromator. DTA-TG curves of materials were performed on a MAC science thermal analyzer (System 001 200 TG-DTA) at a heating rate of 10 °C min^{-1}. Infrared spectra were obtained by a KBr pellet method using a Perkin Elmer system 2000 spectrophotometer. SEM and TEM observations were carried out using a Hitachi type S-2460N natural scanning electron microscope and JEOL type JEM-3010 transmission electron microscope, respectively.

pH Titration

Delithiated material (100 mg) was immersed in 10 cm^3 of a mixed aqueous solution (0.1 M MCl+MOH, M = Li$^+$, Na$^+$ and K$^+$) at varying ratios with intermittent shaking at room temperature for 1 week. After attainment of equilibrium, the pH of the solution was measured with a pH meter.

Distribution coefficient (K_d)

Delithiated material (100 mg) was immersed in 10 cm^3 of solution containing 10^{-4} M of alkali metal ions at different pH with intermittent shaking at room temperature for 1 week. After the attainment of equilibrium, the concentration of alkali metal ions in the supernatant solution was determined by atomic absorption spectrometry and the pH of the solution was measured. The metal ion uptake was calculated from the decrease in the metal ion concentration relative to the initial concentration of the solution used. The K_d value was calculated using the following formula:

K_d (cm^3 g^{-1}) = ion uptake (mg g^{-1} material)/ion concentration (mg cm^{-3} solution)

Uptake of lithium ions from seawater

The lithium ion adsorption from lithium enriched seawater was carried out by stirring 100 mg of delithiated material in 1 dm^3 of LiCl enriched seawater (Li$^+$ concentration being 5 mg dm^{-3}) for 3 days at room temperature. After attainment of equilibrium, the lithium concentration in the supernatant solution was determined by atomic absorption spectrophotometry. The lithium uptake was calculated from the decrease of the lithium concentration of the supernatant solution.

Results and discussion

Preparation and properties of lithium antimony manganese oxide

First we tried to prepare spinel-type lithium antimony manganese oxide by a conventional solid-phase reaction using a mixture of lithium carbonate, manganese carbonate and antimony trioxide, but did not succeed in producing spinel-type samples. However, the hydrothermal method produced spinel-type lithium manganese oxides in the composition range Sb/Mn < 0.25 (Table 1). XRD patterns of LiSbMnO-RT, LiSbMnO-400 and LiSbMnO-600 are given in Fig. 1 (bottom). All the diffraction peaks can be assigned to those of the spinel phase; peaks corresponding to $LiSbO_3$ or $LiSb(OH)_6$ were not observed. These impurity phases were formed as impurities in the compositional region Sb/Mn > 0.25. The lattice constants of all three samples are a little larger than those for spinel-type lithium manganese oxides (8.25 Å for $LiMn_2O_4$ and 8.19 Å for $Li_{1.33}Mn_{1.67}O_4$) (Table 2). The larger lattice constant can be ascribed to the relatively large ionic size of Sb(v) compared to that of Mn(IV).[33] The larger lattice constant shows that antimony atoms exchange with manganese atoms in the spinel phase and participate in the formation of the crystal network of the spinel structure.

SEM images of LiSbMnO-RT and LiSbMnO-400 show that they consist of aggregates of small crystals. The TEM image shows that the sample LiSbMnO-RT consists of cubic particles of less than 200 nm in size. The electron diffraction patterns
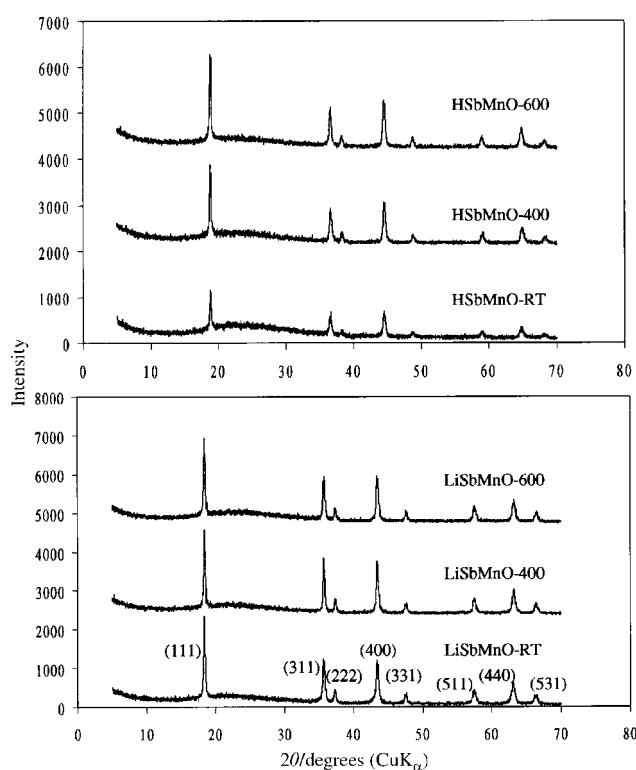

Fig. 1 XRD patterns of lithium antimony manganese oxides (bottom) obtained at different temperatures and their acid treated samples (top).

Table 2 Lattice constants of spinel-type manganese oxides containing various metal ions

Material	Preparation temperature/°C	Li/Mn	M/Mn	Lattice constant/Å	
				Li$^+$ form	H$^+$ form
LiSbMnO-RT	Room temperature	0.75	0.19	8.31 ± 0.01	8.13 ± 0.01
LiSbMnO-400	400	0.75	0.19	8.31 ± 0.01	8.10 ± 0.01
LiSbMnO-600	600	0.75	0.19	8.30 ± 0.01	8.12 ± 0.01
LiMn$_2$O$_4$[a]	800	0.5	—	8.25	8.03
Li$_{1.33}$Mn$_{1.67}$O$_4$[a]	400	0.8	—	8.19	8.06
LiZn$_{0.5}$Mn$_{1.5}$O$_4$[b]	400	0.66	0.33	8.17	8.14
LiZn$_{0.5}$Mn$_{1.5}$O$_4$[b]	600	0.66	0.33	8.20	8.18
LiMg$_{0.5}$Mn$_{1.5}$O$_4$[c]	400	0.66	0.33	8.19	8.14
LiMg$_{0.5}$Mn$_{1.5}$O$_4$[c]	600	0.66	0.33	8.19	8.17
LiAlMnO$_4$[d]	450	1	1	8.14	8.07
LiFeMnO$_4$[d]	450	1	1	8.30	8.30

[a]Ref. 15. [b]Ref. 29. [c]Ref. 30. [d]Ref. 31.

show that the particles are single crystals with a spinel structure. The lattice parameters agree well with those observed in the XRD patterns.

The chemical analysis results for these samples are given in Table 1. Both the Li/Mn and Sb/Mn mole ratios are constant, independent of heating temperature. The mean oxidation numbers (Z_{Mn}) of manganese increases with temperature from 3.50 for LiSbMnO-RT up to 3.54 for LiSbMnO-400 and then 3.56 for LiSbMnO-600, indicating that manganese atoms are in a mixed valence state. A generalized formula for spinel-type lithium antimony manganese oxide can be written as Li$_m$Sb(v)$_x$Mn(III)$_y$Mn(IV)$_z$O$_4$ and the values of m, x, y, and z can be evaluated from the experimental values of Z_{Mn}, Li/Mn and Sb/Mn mole ratios under the condition of electroneutrality as follows:[34]

$$m + 5x + (y+z)Z_{Mn} = 8$$

$$3y + 4z = Z_{Mn}(y+z)$$

$$x = (y+z)(Sb/Mn)$$

$$m = (y+z)(Li/Mn)$$

The chemical formulae for LiSbMnO-RT, LiSbMnO-400, and LiSbMnO-600 are given in Table 1. The heat treatment causes a slight increase in the manganese valence. In addition to electroneutrality, the spinel structure has to fulfill the condition $m + x + y + z = 3$. The calculated values of $(m + x + y + z)$ from the formulae are close to 3, as shown in the last column of Table 1, indicating that the present samples satisfy the general condition for spinel structure, and thus cation deficiencies are not formed. We have simulated the XRD patterns for the ideal formula of the LiSbMnO spinel (Li$_{1.18}$Sb(v)$_{0.30}$Mn$_{1.52}$O$_4$), using the structures of (Li)[Li$_{0.18}$Sb$_{0.30}$Mn$_{1.52}$]O$_4$, (Li$_{0.90}$Sb$_{0.10}$)[Li$_{0.28}$Sb$_{0.20}$Mn$_{1.52}$]O$_4$, with an ordered or disordered Sb, where ( ) and [ ] show tetrahedral and octahedral sites, respectively, in the spinel structure. We concluded from a simulation study of the formula (Li)[Li$_{0.18}$Sb$_{0.30}$Mn$_{1.52}$]O$_4$ that a disordered arrangement of Sb in the 16d site is possible. Thus, the chemical formula for LiSbMnO-RT can be written as (Li)[Li$_{0.16}$Sb(v)$_{0.29}$Mn(III)$_{0.77}$Mn(IV)$_{0.77}$]O$_4$. Similar formulae can be obtained for LiSbMnO-400 and LiSbMnO-600.

Preparation and properties of Li$^+$ extracted samples

More than 99% of lithium in the lithium antimony manganese oxides could be extracted by acid treatment with 0.5 M HCl. The dissolution of a small amount of manganese and antimony took place in addition to the lithium extraction. The amount of dissolved manganese was 12% for LiSbMnO-RT and that of antimony was 2%. The relatively high Mn dissolution is due to the disproportionation reaction of Mn(III) in acidic solution, 2Mn(III)→Mn(II) + Mn(IV), accompanying the Li$^+$ extraction.

Similar dissolution has been observed for LiMn$_2$O$_4$ spinel with trivalent manganese, while it is rarely observed for the Li$_{1.33}$Mn$_{1.67}$O$_4$ spinel with only tetravalent manganese.

The chemical compositions of acid treated samples are shown in Table 1. The Li/Mn ratios are ⩽0.005, while the Sb/Mn ratio increases a little after the acid treatment due to the dissolution of manganese. A characteristic feature is that the mean oxidation numbers of Mn are very close to 4.0 after acid treatment. This shows that the apparent oxidation of manganese progresses during the Li$^+$ extraction, due to the disproportionation reaction of Mn(III) followed by dissolution of Mn(II). The water contents are calculated from the weight loss at 400 °C. The acid treated samples contain a large number of water molecules compared with the other spinel type manganese oxides in the literature.[12,15,29–31]

XRD patterns of acid treated samples show that the extraction of lithium progresses topotactically preserving the spinel structure (Fig. 1, top). The diffraction peaks of LiSbMnO-RT are weakened by the Li$^+$ extraction, while the peak intensities rarely change for LiSbMnO-400 and LiSbMnO-600. Since the fraction of tetravalent manganese increases by heat treatment, we think the metal oxide framework of the spinel structure may become more stable by preheating. The lattice constants decreased from 8.31 ± 0.01 Å to 8.13 ± 0.01 Å. The lattice constants of the present samples and other spinel-type manganese oxides are summarized in Table 2. The lattice constants decrease with Li$^+$ extraction for all samples, but the rate of decrease varies depending upon the starting material. The lithium manganese oxides (LiMn$_2$O$_4$ and LiSbMnO) containing trivalent manganese show a large decrease in the lattice constant with Li$^+$ extraction, due to the oxidation of manganese from trivalent to tetravalent; the ionic radii of manganese are 0.72 Å and 0.67 Å for Mn(III) and Mn(IV), respectively.[33]

The SEM images of the acid treated samples do not show distinguishable differences following acid treatment. The TEM images, however, show that the particle shape changes from a well crystallized cubic form to an irregular shape as a result of the acid treatment, owing to the dissolution of manganese and antimony. The high magnification TEM image for sample HSbMnO-400 shows lattice images in the particles; this indicates that the local spinel structure is preserved after the acid treatment, in spite of some dissolution of manganese and antimony. Similar behavior has been observed in the case of Mg^{2+} extraction from Mg$_2$MnO$_4$; the spinel structure was preserved even after considerable dissolution of MgO.[29]

The DTA-TG curves of HSbMnO-RT are given in Fig. 2. Similar curves were obtained for HSbMnO-400 and HSbMnO-600. The large endothermic peak around 80 °C with weight loss corresponds to the evaporation of adsorbed water. The shoulder around 280 °C with weight loss can be ascribed to the condensation and loss of lattice hydroxyl groups. The large

weight loss around 80 °C shows that a considerable quantity of lattice hydroxyl groups are formed in HSbMnO-RT. A small endothermic peak around 660 °C can be assigned to formation of $MnSb_2O_4$ as evidenced from XRD analysis. An endothermic peak around 550 °C due to the transformation from MnO_2 to Mn_2O_3 was not observed for the present samples. This indicates that the antimony atoms suppress the reduction of manganese from the tetravalent to the trivalent form.

IR spectra of LiSbMnO-RT and HSbMnO-RT are shown in Fig. 3. New peaks around 3300 and 900 cm^{-1} are formed by the lithium extraction from LiSbMnO-RT. These bands can be ascribed to the stretching vibrations of hydroxyl groups and the lattice vibration of hydroxyl groups, respectively.[7,18] They show the formation of lattice hydroxyl groups during the acid treatment.

We have studied the Li$^+$ extraction reactions with $LiMn_2O_4$ and $Li_{1.33}Mn_{1.67}O_4$ in detail.[13,15] In the $LiMn_2O_4$ spinel, a redox type extraction reaction progresses and tetrahedral vacant sites form after Li$^+$ extraction, while in $Li_{1.33}Mn_{1.67}O_4$, an ion exchange type extraction progresses and lattice proton sites form. The present samples show different extraction behavior from these two cases. The extraction reaction progresses by the redox type reaction, but lattice protons form instead of tetrahedral vacant sites. This suggests that the disproportionation reaction takes place throughout the particle preserving the spinel structure, in contrast to $LiMn_2O_4$ where the disproportionation reaction occurs only at the surface of particles since it belongs to a one-phase solid solution system. The presence of a large amount of adsorbed water suggests that the disproportionation reaction takes place inside the particle in the present samples and some water molecules may participate in the formation of the hydroxyl groups at the tetrahedral sites of manganese oxide.

Distribution coefficient

The equilibrium distribution coefficients (K_d) of alkali metal ions on HSbMnO-RT were measured at different pH values (Fig. 4). The selectivity sequence of alkali metal ions is in the order Na < Li < K < Rb < Cs in acidic solution; high selectivity for Li$^+$ was not observed. A similar selectivity sequence has been observed for the spinel-type manganese oxide obtained by the acid treatment of $Mg_2Mn_2O_4$ although it shows a lithium ion-sieve property in alkaline solutions.[35] Since the distribution coefficient reflects the ion selectivity at micro-loading, the present results suggest that there are a small number of ion exchange sites which are selective to Cs$^+$ and which have relatively strong acidity. The slopes of dlog K_d/dpH are nearly 1 indicating an ideal 1 : 1 ion exchange reaction.

The pH titration study

The pH titration curves were obtained by adding the acid treated sample to the alkali metal hydroxide solutions in
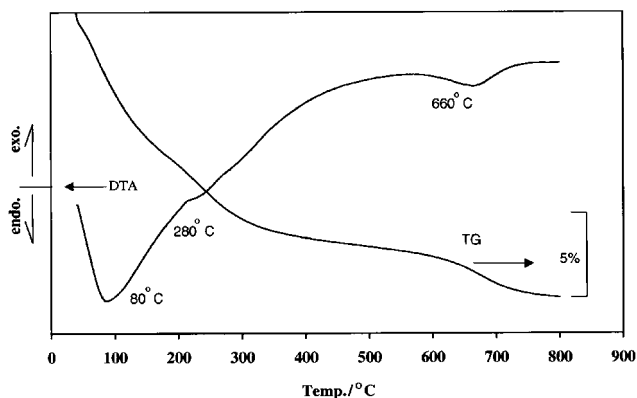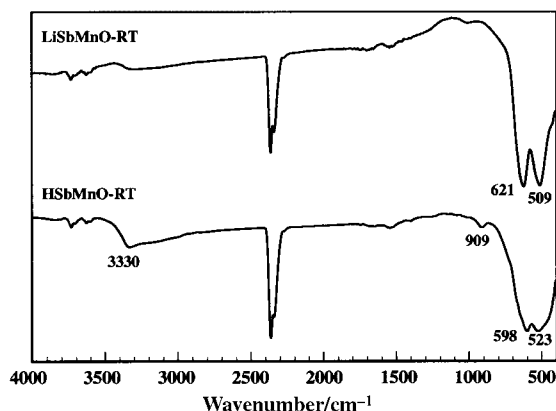

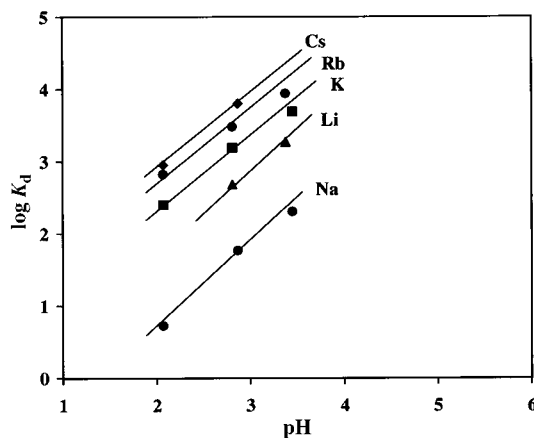Fig. 3 IR spectra of LiSbMnO-RT and HSbMnO-RT.

Fig. 4 Distribution coefficients of alkali metal ions in HSbMnO-RT as a function of pH. Adsorbent: 0.10 g, vol.: 10 cm^3, initial concentration: 10^{-4} M.

different concentrations, followed by pH measurement. The supernatant solution remained colorless for all samples, even in 0.1 M LiOH solution. This indicates that only a Li$^+$/H$^+$ ion exchange reaction takes place, and that vacant tetrahedral sites do not form in the present samples. When the vacant tetrahedral sites are present, the redox type insertion reaction takes place and the color of the supernatant solution changes to purple-red due to the formation of MnO_4^- ions. The pH titration curves of HSbMnO-RT, HSbMnO-400, and HSbMnO-600 towards lithium, sodium and potassium ions are shown in Fig. 5. The titration curves resemble each other regardless of heating temperature and demonstrate a remarkably large exchange capacity towards lithium ions, showing that they have lithium ion-sieve properties. The exchange capacities of HSbMnO-RT are 5.6 mmol g^{-1} for Li$^+$, and 0.8 mmol g^{-1} for Na$^+$ and K$^+$. The exchange capacity for Li$^+$ is close to the value expected (6.1 mmol g^{-1}) from the chemical composition of LiSbMnO-RT.

The selectivity coefficient (K_c) for the Li$^+$/H$^+$ exchange can be evaluated from the pH titration data as follows:[36]

$$pK_c = -\log K_c = pH - \log \{\alpha/(1-\alpha)\} + \log C_{Li}$$

where α is the degree of neutralization and C_{Li} is the lithium concentration in the supernatant solution. The pK_c values for the present samples are plotted as a function of α in Fig. 6. The pK_c vs. α curves for the spinel-type manganese oxides with redox and ion-exchange sites are also given as dotted lines in the same figure, using the pH titration data in the literature.[15] The pK_c vs. α curves for HSbMnO-RT resembled that for ion-exchange type manganese oxide ($MnO_2 \cdot 0.31H_2O$), while the pK_c values are considerably lower than those for a redox type sample (λ-MnO_2). This shows that the acidity of the present
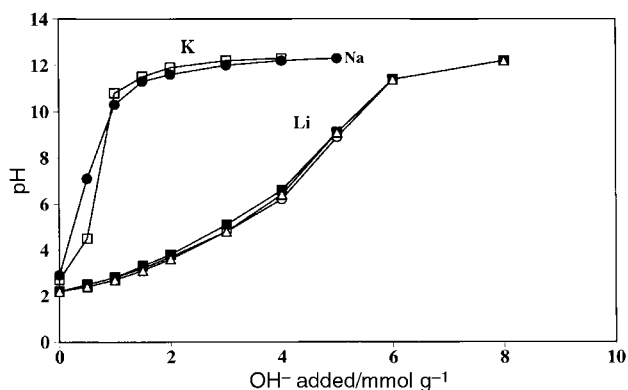

Fig. 2 DTA-TG curves of HSbMnO-RT.

Fig. 5 The pH titration curves towards lithium, sodium and potassium ions. HSbMnO-RT: ○, ●, □; HSbMnO-400: ■; HSbMnO-600: △.
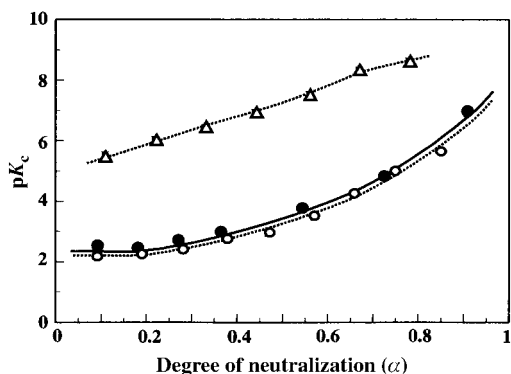

Fig. 6 The pK_c vs. α curves for Li^+/H^+ exchanges in HSbMnO-RT. Dotted curves are calculated from the pH titration curves of spinel-type manganese oxide in ref. 15. λ-MnO_2: △, HSbMnO-RT: ●, $MnO_2 \cdot 0.31 H_2O$: ○.

sample is stronger than that of the redox type spinel, while nearly equal to that for the ion-exchange type spinel. The highly acidic property of the present sample is advantageous for the recovery of lithium from a weakly basic solution like seawater.

Lithium uptake from LiCl-enriched seawater

Lithium adsorptive properties of delithiated materials in a LiCl-enriched seawater were studied batchwise at 25 °C. They showed the selective adsorption of lithium even from seawater containing an extremely large quantity of sodium ions. The lithium uptakes were 14, 12 and 11 mg g^{-1} for HSbMnO-RT, HSbMnO-400, and HSbMnO-600, respectively. These values are higher than those for other kinds of lithium selective adsorbent containing antimony, such as tin antimonate,[37] titanium antimonate[38] or monoclinic type antimonic acid.[39]

Conclusion

Spinel-type lithium manganese oxide containing pentavalent antimony atoms can be synthesized by hydrothermal reaction in the compositional range Sb/Mn < 0.25. It has a unique chemical formula containing Mn(III), Mn(IV) and Sb(V), with a lattice constant (8.31 ± 0.01 Å) larger than those of spinel-type lithium manganese oxides only. Most of the lithium in the solid can be extracted by acid treatment, preserving the spinel structure. The acid treated material shows excellent lithium

ion-sieve properties during the ion exchange reaction in the aqueous phase.

References

1 C. B. Amphlett, *Inorganic Ion Exchangers*, Elsevier Publishing Co., Amsterdam, 1964.
2 A. Clearfield ed., *Inorganic Ion Exchange Materials*, CRC Press, Boca Raton, FL, 1982.
3 R. M. Barrer, *Zeolite and Clay Minerals as Sorbents and Molecular Sieves*, Academic Press Inc., London, 1978.
4 M. Abe, in *Ion Exchange and Solvent Extraction*, J. A. Marinsky and Y. Marcus eds., Marcell Dekker, Inc., New York, 1995, vol. 12, p. 381.
5 G. Alberti, U. Costantino, S. Ali and N. Tomassini, *J. Inorg. Nucl. Chem.*, 1978, **40**, 1113.
6 Q. Feng, H. Kanoh and K. Ooi, *J. Mater. Chem.*, 1999, **9**, 319.
7 V. V. Vol'khim, G. V. Leont'eva and S. A. Onorin, *Neorg, Mater.*, 1973, **9**, 1041.
8 J. C. Hunter, *J. Solid State Chem.*, 1981, **39**, 142.
9 X. M. Shen and A. Clearfield, *J. Solid State Chem.*, 1986, **4**, 270.
10 K. Ooi, Y. Miyai and S. Katoh, *Sep. Sci. Technol.*, 1986, **21**, 755.
11 Y. Onodera, T. Iwasaki, H. Hayashi and K. Torri, *Chem. Ind.*, 1989, **20**, 108.
12 R. Chitrakar and M. Abe, *Mater. Res. Bull.*, 1988, **23**, 1231.
13 K. Ooi, Y. Miyai, S. Katoh, H. Maeda and M. Abe, *Langmuir*, 1989, **5**, 150.
14 K. Ooi, Y. Miyai, S. Katoh, H. Maeda and M. Abe, *Langmuir*, 1990, **6**, 289.
15 Q. Feng, Y. Miyai, H. Kanoh and K. Ooi, *Langmuir*, 1992, **8**, 1861.
16 H. Kanoh, Q. Feng, Y. Miyai and K. Ooi, *J. Electrochem. Soc.*, 1993, **140**, 3162.
17 H. Kanoh, Q. Feng, Y. Miya and K. Ooi, *J. Electrochem. Soc.*, 1995, **142**, 702.
18 B. Ammundsen, D. J. Jones, J. Roziere and G. R. Burns, *Chem. Mater.*, 1995, **7**, 2151.
19 B. Ammundsen, D. J. Jones and J. Roziere, *Chem. Mater.*, 1998, **10**, 1680.
20 B. Ammundsen, J. Roziere and M. S. Islam, *J. Phys. Chem. B*, 1997, **101**, 8156.
21 Y. J. Lee, F. Wang and C. L. Grey, *J. Am. Chem. Soc.*, 1998, **120**, 12601.
22 J. B. Goodenough, M. M. Thackery, W. I. F. David and P. G. Bruce, *Rev. Chim. Miner.*, 1984, **21**, 435.
23 T. Ohzuku, M. Kato, K. Sawai and T. Hirai, *J. Electrochem. Soc.*, 1991, **138**, 2556.
24 M. M. Thackeray, *J. Am. Ceram. Soc.*, 1999, **82**, 3347.
25 K. Ooi, Y. Miyai and S. Katoh, *Sep. Sci. Technol.*, 1987, **22**, 1779.
26 Y. Miyai, K. Ooi and S. Katoh, *Sep. Sci. Technol.*, 1988, **23**, 179.
27 R. Khamizov, D. N. Muraviev and A. Warshawsky, in *Ion Exchange and Solvent Extraction*, J. A. Marinsky and Y. Marcus eds., Marcel Dekker, Inc., New York, 1995, vol. 12, p. 93.
28 Y. Miyai, K. Ooi, T. Nishimura and J. Kumamoto, *Bull. Soc. Sea Water Sci. Jpn.*, 1994, **48**, 414 (in Japanese).
29 Q. Feng, Y. Miyai, H. Kanoh and K. Ooi, *Chem. Mater.*, 1993, **5**, 311.
30 Q. Feng, H. Kanoh, Y. Miyai and K. Ooi, *Chem. Mater.*, 1995, **7**, 379.
31 Y. Liu, Q. Feng and K. Ooi, *J. Colloid Interface Sci.*, 1994, **163**, 130.
32 Japan Industrial Standard (JIS), 1969, M8233.
33 R. D. Shannon, *Acta Crystallogr., Sect. A*, 1976, **32**, 751.
34 E. Pollert, *Prog. Cryst. Growth Charact.*, 1984, **9**, 263.
35 Y. Miyai, K. Ooi and S. Katoh, *J. Colloid Interface Sci.*, 1989, **103**, 535.
36 K. Ooi, Y. Miyai, S. Katoh, H. Maeda and M. Abe, *Bull. Chem. Soc. Jpn.*, 1988, **61**, 407.
37 M. Abe and K. Hayashi, *Hydrometallurgy*, 1983, **12**, 83.
38 M. Abe and R. Chitrakar, *Hydrometallurgy*, 1987, **16**, 117.
39 M. Abe, R. Chitrakar and M. Tsuji, *Chem. Ind. (Tokyo)*, 1989, **42**, 1224 (in Japanese).